Profiling p^+/n-Well Junction by Nanoprobing and Secondary Electron Potential Contrast

Po-Tsun Liu, *Senior Member, IEEE*, and Jeng-Han Lee

***Abstract*—This letter investigates the use of secondary electron potential contrast (SEPC) with an *in situ* dynamic nanoprobing trigger to examine a silicon p^+/n-well junction. Experimental results demonstrate that applying a bias to the p^+/n-well junction nodes can intensify the SEPC signal. An image processing procedure is used to convert the image contrast to a voltage scale, allowing the depletion region to be identified. The proposed method can maintain stable voltage conditions in the junction, facilitating inspection of the dopant area by scanning electron microscopy, potentially contributing to the development of an efficient method for examining dopant areas in real circuits.**

***Index Terms*—Junction profiling, nanoprobing, scanning electron microscope (SEM), secondary electron potential contrast (SEPC).**

I. Introduction

THE PERFORMANCE of a semiconductor device is controlled by the distribution and concentration of the dopant. Several approaches have been developed for inspecting the 2-D dopant profile of semiconductor junctions. Secondary ion mass spectrometry (SIMS) is extensively used to obtain dopant profiles with effective quantization. However, this method provides only 1-D information on a specific test key structure [1], [2]. Chemical delineation using acid solutions can yield 2-D dopant profiles in the active region where the implant dosage is high [3]–[5]. This method, however, cannot easily inspect the dopant profile of a well region clearly because it uses low dopant dosage. Scanning capacitance microscopy (SCM) is another popular method for acquiring a 2-D dopant profile. A high-quality oxide layer must be grown on silicon wafers to enable a reliable quantitative measurement, increasing the complexity of the SCM.

Recently, secondary electron potential contrast (SEPC) in scanning electron microscope (SEM) has emerged as a potential method for dopant profile inspection, with a sensitivity from 10^{16} to 10^{20} cm^{-3} and a spatial resolution of 10 nm [6], [7]. When the device of interest has nanoscale dimensions, spatial resolution, site-specific analytical capability, and SEPC signal enhancement are the three most important issues in the SEPC method [8], [9]. Jepson *et al.* observed that the SEPC spatial resolution is improved in helium ion microscopy (HeIM), in which a probe size as small as 0.25 nm can be used, making HeIM an ideal candidate for nanoscale dopant mapping in the future [10], [11]. Kazemian *et al.* proposed the preparation of a sample using a focused ion beam (FIB) to meet the requirements for site-specific analysis [12]. However, little literature has been published on SEPC signal enhancement. Moreover, the preparation of a FIB sample produces an amorphous surface layer and reduces the SEPC of the SEM image [12]. Additionally, the SEPC signal arises from the built-in potential across the diode. The drop in SEPC signal reduction is expected to be even worse for semiconductors with a smaller bandgap energy. In the worse case, no SEPC image contrast will be observed, limiting the application of the SEPC method to small bandgap material like silicon. In this letter, an *in situ* dynamic trigger is developed to intensify the SEPC signal of p^+/n-well junctions, with a view to extending SEPC to the real circuits of silicon.

Manuscript received March 28, 2011; revised April 14, 2011; accepted April 14, 2011. Date of publication May 19, 2011; date of current version June 29, 2011. The review of this letter was arranged by Editor C. Bulucea.

P.-T. Liu is with the Department of Photonics and Display Institute, National Chiao Tung University, Hsinchu 30010, Taiwan (e-mail: ptliu@mail.nctu.edu.tw).

J.-H. Lee is with the Department of Photonics and Institute of Electro-Optical Engineering, National Chiao Tung University, Hsinchu 30010, Taiwan (e-mail: jameslee395@gmail.com).

Color versions of one or more of the figures in this letter are available online at http://ieeexplore.ieee.org.

Digital Object Identifier 10.1109/LED.2011.2147752

II. Experiment

The specimen in this letter was a static random access memory (SRAM) that was manufactured using 90-nm IC technology on a p-type (100) Si wafer. After the active area was patterned, phosphorous and boron dopants were implanted into the silicon wafer to form n- and p-wells, respectively. Then, p^+-type source and drain regions were formed by boron implantation, and arsenic was implanted to form n^+-type source and drain regions. Thermal activation and metallization were conducted in that order following the formal procedures. The cross section of the SRAM chip was manually polished for SEPC inspection using a Hitachi S4800 SEM. The SEPC image was obtained using an accelerating energy of 1 kV and a working distance of 6 mm. To intensify the SEPC signal, a Klocke Nanotechnik nanoprobing system with three micromanipulators was used to apply a reverse bias to the junction, which was mounted on the stage of the Hitachi S4800. Fig. 1 shows the partial cross section of the SRAM chip to illustrate the SEPC inspection; three p^+/n-well junctions and two polycrystalline Si gates are shown, and a pair of nanoprobing tips was inserted on the rightmost p^+/n-well junction.

III. Results and Discussion

Fig. 2 shows the SEM image that corresponds to Fig. 1. An SEPC signal is clearly observed on the rightmost

0741-3106/$26.00 © 2011 IEEE

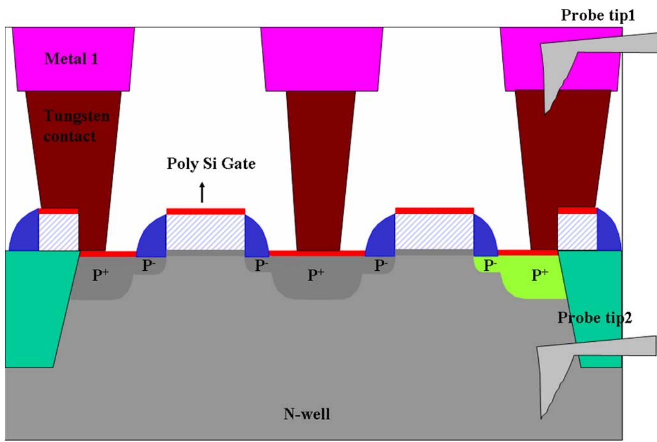

Fig. 1. Partial cross section of the SRAM chip to illustrate the SEPC inspection; three p^+/n-well junctions and two polycrystalline Si gates are shown. A pair of nanoprobing tips was inserted on the rightmost p^+/n-well junction, in which the green color represents the SEPC signal when the probe tips were electrically biased with a trigger voltage of −1 V on the p^+ side and 0 V on the n-well side.

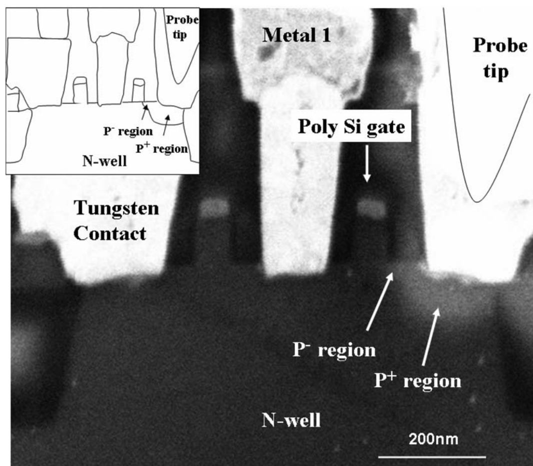

Fig. 2. SEM image corresponds to Fig. 1. An SEPC signal is clearly observed on the rightmost p^+/n-well junction when the probe tips were electrically biased with a trigger voltage of −1 V on the p^+ side and 0 V on the n-well side. In contrast, no SEPC signal is observed at the other two pairs of p^+/n-well junctions that were not probed by the nanotips in this figure. The corresponding schematic cross section is shown in the inset of this figure.

p^+/n-well junction when the probe tips were electrically biased with a trigger voltage of −1 V on the p^+ side and 0 V on the n-well side. In contrast, no SEPC signal is observed at the other two pairs of p^+/n-well junctions that were not probed by the nanotips in Fig. 2. This result is attributable to the fact that a semiconductor junction with a small energy bandgap cannot easily be examined using the standard SEPC approach. Moreover, the method that is presented in this letter provides a good spatial resolution, even for an image of a lightly doped drain region (p^- region).

A p^+/n-well junction consists of three regions: a p^+ region, a depletion region, and a well region. The p^+ and n-well regions are maintained at a steady voltage because their resistivity is lower than that of the depletion region and most of the reversed voltage is across the depletion region. Elliott *et al.* found that the SEPC intensity of a sample is proportional to the potential of the silicon surface [7]. Therefore, the image

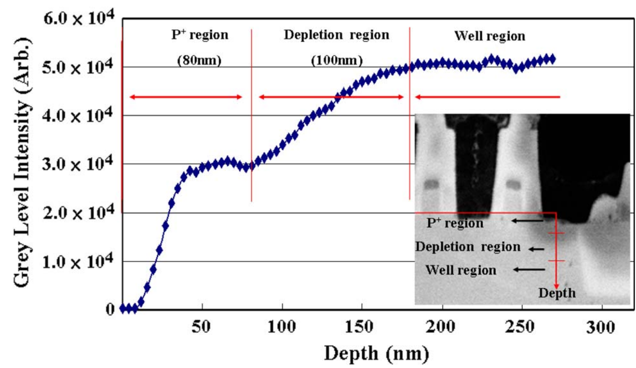

Fig. 3. Intensity profile of p^+/n-well junction after applying a series of image processing procedures. The corresponding image is shown in the inset of this figure. Three regions, a p^+ region, a depletion region, and a well region, were labeled on this chart. The depths of p^+ and depletion regions were measured, and their values are 80 and 100 nm, respectively.

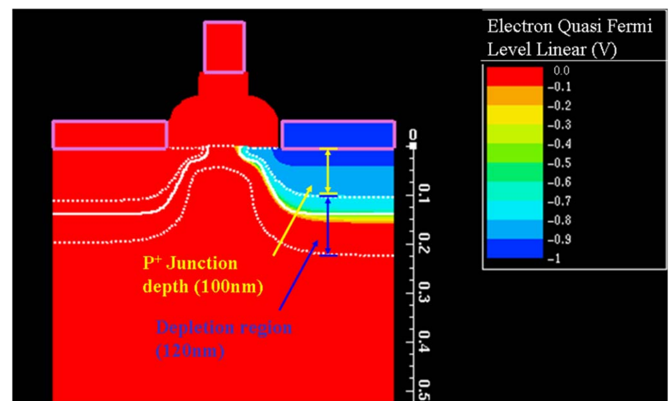

Fig. 4. Voltage distribution map of p^+/n-well junction, simulated by device simulator Silvaco TCAD as set by a voltage of −1 V on the p^+ side and 0 V on the n-well side. Simulation result shows that the depth of the p^+ region and the depletion width are 100 and 120 nm, respectively.

intensity simply reflects the potential of the sample, to which it is proportional. To obtain more information on the physics of the device, the image processing in Fig. 2 was applied. Fig. 3 shows the intensity profile of the p^+/n-well junction that is obtained by a series of image processing procedures. The reverse tone processing in Fig. 2 was performed first, and the inset in Fig. 3 shows the results: The highlighted vertical red line represents the location used for intensity profile extraction. Every point in the intensity profile is an average over a point and its four adjacent points. Three regions are shown in Fig. 3. In the p^+ region, the sharp increase in the intensity reflects the contact that was made with the tungsten plug. It is followed by a gentle rise to a steady brightness with an intensity of 3.0×10^4. Thereafter, the intensity increases gradually, representing the depletion region of the p^+/n-well junction. Finally, a steady intensity of 5.0×10^4 is observed, representing the well region. The depths of the p^+ and depletion regions were measured to be 80 and 100 nm, respectively, closely matching the designed depth.

SIMS is an excellent tool for analyzing dopant depth profiles on a specific test key structure. In the lack of an adequate 2-D dopant profiling method, some semiconductor manufacturing companies use SIMS depth profiles to calibrate 2-D technology computer-aided design (TCAD) process simulators. Fig. 4

shows the 2-D voltage distribution for a biased p^+/n-well junction obtained using the Silvaco TCAD process simulator, which is calibrated by a SIMS depth profile. The results of the simulation indicate that the p^+ junction depth and depletion width are 100 and 120 nm, respectively, exceeding the values measured by the SEPC method. These results reveal the inadequacy of the simulator calibration flow, in which characterization is based on the SIMS depth profile.

IV. Conclusion

In summary, a novel combination of nanoprobing and SEPC has been proposed to investigate a silicon p^+/n-well junction. Experiment results demonstrate that *in situ* nanoprobing can enhance the SEPC signal. In contrast, no SEPC signal is observed on the junctions that were not electrically biased by nanotips. The present findings confirm that the SEPC signal arises from the surface potentials across the diode. The discrepancy between SEPC results and simulation results reveals the demand of a 2-D dopant profiling method for calibration of TCAD process simulators. This letter potentially provides a simple and efficient procedure that enables a 2-D junction profile to be obtained in a real transistor device. Future research is therefore necessary to characterize the 1-D spatial resolution and dopant concentration sensitivity of the method with well-established techniques like SIMS and high-resolution spreading resistance probe.

Acknowledgment

The authors would like to thank the editor and reviewers for reading this letter and offering a number of helpful comments and Y. T. Lin, Y. S. Huan, D. Su, C. C. Wu, and E. Hsu for their kind support and valuable discussions.

References

[1] A. F. Tasch, H. Shin, C. Park, J. Alvis, and S. Novak, "An improved approach to accurately model shallow B and BF2 implants in silicon," *J. Electrochem. Soc.*, vol. 136, no. 3, pp. 810–814, 1989.

[2] Y. Naitou and N. Ookubo, "Shear-mode scanning capacitance microscope," *Appl. Phys. Lett.*, vol. 78, no. 19, pp. 2955–2957, May 2001.

[3] M. Barrett, M. Dennis, D. Tiffin, Y. Li, and C. K. Shih, "2-D dopant profiling in VLSI devices using dopant-selective etching: An atomic force microscopy study," *IEEE Electron Device Lett.*, vol. 16, no. 3, pp. 118–120, Mar. 1995.

[4] C. J. M. Eijkel, J. Branebjerg, M. Elwenspoek, and F. C. M. Van de pol, "A new technology for micromachining of silicon: Dopant selective HF anodic etching for the realization of low-doped monocrystalline silicon structures," *IEEE Electron Device Lett.*, vol. 11, no. 12, pp. 588–589, Dec. 1990.

[5] C. J. Choi, T. Y. Seong, K. M. Lee, J. H. Lee, Y. J. Park, and H. D. Lee, "Abnormal junction profile of silicided p^+/n shallow junctions: A leakage mechanism," *IEEE Electron Device Lett.*, vol. 23, no. 4, pp. 188–190, Apr. 2002.

[6] D. Venables and D. M. Maher, "Quantitative two-dimensional dopant profiles obtained directly from secondary electron images," *J. Vac. Sci. Technol. B, Microelectron. Nanometer Struct.*, vol. 14, no. 1, pp. 421–425, Jan. 1996.

[7] S. L. Elliott, R. F. Broom, and C. J. Humphreys, "Dopant profiling with the scanning electron microscope—A study of Si," *J. Appl. Phys.*, vol. 91, no. 11, pp. 9116–9122, Jun. 2002.

[8] D. Venables, H. Jain, and D. C. Collins, "Secondary electron imaging as a two-dimensional dopant profiling technique: Review and update," *J. Vac. Sci. Technol. B, Microelectron. Nanometer Struct.*, vol. 16, no. 1, pp. 362–366, Jan. 1998.

[9] A. C. Diebold, M. R. Kump, J. J. Kopanski, and D. G. Seiler, "Characterization of two-dimensional dopant profiles: Status and review," *J. Vac. Sci. Technol. B, Microelectron. Nanometer Struct.*, vol. 14, no. 1, pp. 196–201, Jan. 1996.

[10] M. A. E. Jepson, B. J. Inkson, C. Rodenburg, and D. C. Bell, "Dopant contrast in the helium ion microscope," *Europhys. Lett.*, vol. 85, no. 4, p. 46 001, Feb. 2009.

[11] M. A. E. Jepson, B. J. Inkson, X. Liu, L. Scipioni, and C. Rodenburg, "Quantitative dopant contrast in the helium ion microscope," *Europhys. Lett.*, vol. 86, no. 2, p. 26 005, Apr. 2009.

[12] P. Kazemian, A. C. Twitchett, C. J. Humphreys, and C. Rodenburg, "Site-specific dopant profiling in a scanning electron microscope using focused ion beam prepared specimens," *Appl. Phys. Lett.*, vol. 88, no. 21, p. 212 110, May 2006.